ISSN 1392–1320 MATERIALS SCIENCE (MEDŽIAGOTYRA). Vol. 16, No. 3. 2010

Investigation of the Electrical Characteristics of the Metal / Organic Semiconductor / Metal Structures with Top Contact Configuration

Šarūnas MEŠKINIS [1], Kęstutis ŠLAPIKAS [1], Rimas GUDAITIS [1], Sigitas TAMULEVIČIUS [1], Aleksandras ILJINAS [1], Angelė GUDONYTĖ [1], Juozas Vidas GRAŽULEVIČIUS [2], Vytautas GETAUTIS [2], Asta MICHALEVIČIŪTĖ [2], Tadas MALINAUSKAS [2], Ramūnas LYGAITIS [2]

[1] *Institute of Materials Science of Kaunas University of Technology, Savanorių 271, LT-50131 Kaunas, Lithuania*
[2] *Faculty of Chemical Technology, Kaunas University of Technology, Radvilėnų 19, LT-50254 Kaunas, Lithuania*

Received 29 July 2009; accepted 16 September 2010

In present study four newly synthesized organic semiconductor compounds have been used for fabrication of the planar metal / organic semiconductor / metal structures. I-V characteristics of the samples were investigated. Effect of the hysteresis of the I-V characteristics was observed for all samples investigated. However, strength of the hysteresis depended on organic semiconductor used. Charge transfer mechanisms were considered. In all cases the main charge transfer mechanism was trap activated tunneling. Yet at higher electric fields Schottky emission should be considered as well.
Keywords: organic semisonductor, metal-semiconductor contacts, spin coating, current-voltage characteristics, charge transport mechanisms.

1. INTRODUCTION

Organic semiconductors are at the top of the considerable interest due to the possibility to make electronic devices on flexible materials (for example plastic or paper) using cheap technological processes such as spin coating and printing [1 – 4]. In order to improve efficiency of an organic semiconductor device, it is important to have a comprehensive knowledge of charge transport mechanism, because it is one of the main factors affecting the device characteristics. Particularly electrical properties of the metal / organic semiconductor contacts are under intensive investigations, because understanding of the basic transport mechanisms in these junctions is very helpful in distinguishing between the influence of the interfacial and bulk effects on electrical properties of the organic semiconductor based devices. Such information would help to select the most problematic parts of the organic semiconductor devices and ways for optimization of the device fabrication technology. In such a way improvement of the functional characteristics of the organic semiconductor based electronic devices such as organic field effect transistors (OFET), organic solar cells, organic light emitting diodes would be achieved.

In present research, current-voltage (I-V) characteristics of the metal / organic semiconductor / metal structures fabricated using the four new organic semiconducting compounds were investigated. Charge transport mechanisms in metal / organic semiconductor / metal structures were studied.

2. EXPERIMENTAL

In the present study top-contact configuration of the samples has been used (Fig. 1). Monocrystalline wafers with thermally grown silicon dioxide (SiO_2) layers on the top were used as a readily available substrates. Before deposition of the organic semiconductor layer the substrates were degreased in dimethylformamide and acetone. Afterwards organic semiconductor thin films were deposited by spin coating (deposition conditions are presented in Table 1).

Formation of the samples was finished by vacuum evaporation of the metal electrodes. 300 nm thickness Al, Au, Cr and Ti films were deposited through the mask. In most experiments square-shaped electrodes were applied (Fig. 1).

Four organic semiconductors were investigated in the present study:

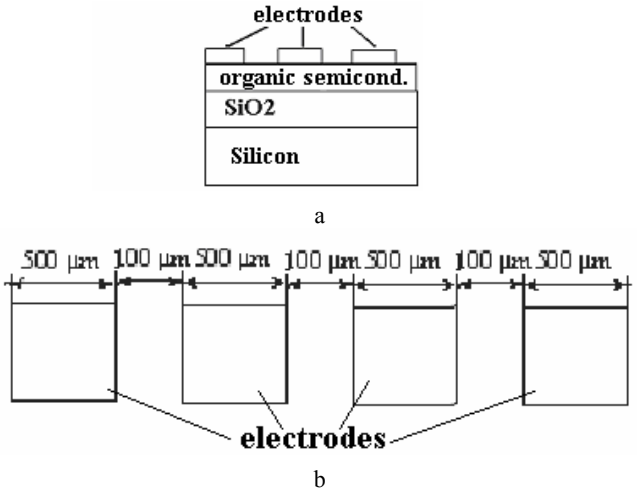

Fig. 1. Structure of the metal / organic semiconductor / metal samples used in present study: cross-section (a) and top view (b)

- 4,4'-diformyltriphenylamine bis(N-2,3-epoxypropyl-N-phenylhydrazone) (further in the present study MT-12);
- Di(2,2-diphenylvinyl)(9-ethyl-3-carbazolyl)amine (further in the present study E-139);

*Corresponding author. Tel.: +370-37-327605; fax: +370-37-314423.
E-mail address: *sarunas.meskinis@fei.lt* (Š. Meškinis)

- 4-diphenylaminobenzaldehyde N-methyl-N-phenylhydrazone (further in the present study AT-RB-1);
- 4-diphenylaminobenzaldehyde N,N-diphenylhydrazone (further in the present study AT-RB-2);

The synthesis of the organic semiconductor MT-12 were reported earlier [5]. The synthesis and characterization of E-139 are presented in [7]. The synthesis of AT-RB-1 and AT-RB-2 has been described by Nomura et al in [6]. All organic semiconductors had p-type conductivity. The structures of organic semiconductors used in this study are shown below (Fig. 2).

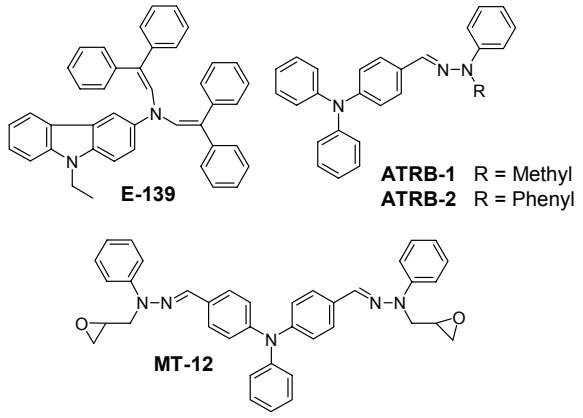

Fig. 2. The structures of the organic semiconductors used in the present study

All organic semiconductor materials used in the present study form glasses. The glass transition temperatures of MT-12, AT-RB-1, AT-RB-2, and E-139 were determined to be 65 °C, 30 °C, 50 °C and 104 °C, respectively [5 – 7]. Therefore in some cases deposited organic semiconductor layers were air annealed at 100 °C temperature to investigate possible influence of the glass phase formation on electrical properties of the metal / / organic semiconductor structures.

Thickness of the spin coated organic semiconductor films was measured by a laser ellipsometer Gaertner L115 ($\lambda = 633$ nm). Current-voltage characteristics of the organic field effect transistors were investigated using a picoammeter/voltage source Keithley 6487. The measurements were performed in nitrogen gas ambient.

Table 1. Parameters of the organic semiconductor thin film deposition process

Organic semicond.	Solvent	Solution formation temp.	Concentr. of the solution (%)	Spin coat. rate (rpm)	Thickn. of the layer (nm)
AT-RB-1	THF*	Room	5	6000	178
AT-RB-2	THF*	Room	5	6000	162
E-139	THF*	Room	3	8000	170
MT-12	THF*	+40 °C	5	6000	168

* THF refers to the tetrahydrofurane.

Different charge transfer mechanisms in metal / organic semiconductor contacts were considered in present research. To define possible charge transfer mechanisms both contact limited (Schottky emission, Fowler-Nordheim emission, trap activated tunnelling) and bulk limited (space charge limited current, Poole-Frenkel emission) mechanisms were investigated.

Schottky emission (current flow over the potential barrier at the metal/semiconductor contact) is described by the following equation [8]:

$$J = A^* T^2 \exp\left(\frac{\beta_S E^{1/2} - q\varphi_B}{kT}\right), \quad (1),$$

where J is the current density, $\beta_S = (q^3/4\pi\varepsilon_0\varepsilon)^{1/2}$, A^* – effective Richardson constant, q – electron charge, ε_0 – vacuum dielectric permittivity, k – Boltzmann constant, T – temperature, φ_B – Schottky contact potential barrier height, ε – organic semiconductor dielectric permittivity. Thus presence of the Schottky emission can be identified from the linear dependence of $\ln(J) \sim E^{1/2}$. Presence of that charge transfer mechanism can be checked by comparison of the dielectric permittivity calculated from the (1) equation with dielectric permittivity calculated from the capacitance-voltage measurement data, too.

Fowler-Nordheim tunnelling is described by the following equation: [8]

$$J = \frac{m}{m^*}\frac{q^3}{8\pi h\phi}E^2 \exp\left(\frac{-B}{E}\right), \quad (2),$$

where m is the electron mass, m^* – electron effective mass, h – Plank constant, ϕ – potential barrier height. Presence of the Fowler-Nordheim charge transfer mechanism can be identified from the linear dependence of $\ln(J/E^2) \sim E^{1/2}$.

Trap assisted tunnelling via traps at the metal/organic semiconductor interface is described by $\ln(J) \sim 1/E$ dependence [9].

Space charge limited current is related with accumulation of the space charge in bulk of the semiconductor [8]. It can be described by the $\log(J) \sim \log V$ ($\log(J) \sim \log(E)$) dependence. In such a case current density is dependent on the distance between the electrodes: the higher distance the lower current density will be detected.

Poole-Frenkel emission is related to trapping of the charge carriers by local traps related with bulk defects and subsequent release of the trapped charge carriers from these potential wells [8]. Poole-Frenkel emission can be described by following equation:

$$J = J_0 \exp\left(\frac{\beta_{PF} E^{1/2} - q\varphi_{PF}}{kT}\right), \quad (3)$$

where $\beta_{PF} = (q^3/4\pi\varepsilon_0\varepsilon)^{1/2}$. The Poole-Frenkel emission can be identified by known dependence of the relation $\ln(J/E) \sim E^{1/2}$. Presence of that charge transfer mechanism can be checked by comparison of the dielectric permittivity calculated from the equation (4) with the dielectric permittivity calculated from the capacitance-voltage measurement data, too.

3. EXPERIMENTAL RESULTS

3.1. Peculiarities of the current-voltage characteristics and I-V hysteresis effects

Typical current-voltage characteristics of the metal / / organic semiconductor (AT-RB-1) contacts are presented in Fig. 3. In all cases no clear relation between the electrode metal workfuntion (Table 2) and I-V

characteristics of the metal / organic semiconductor contacts were observed.

Current-voltage characteristics of all the samples investigated can be divided into two groups. The only exclusion are samples fabricated using organic semiconductor AT-RB-2 (Fig. 4). In this case the large scattering of the measured characteristics was detected.

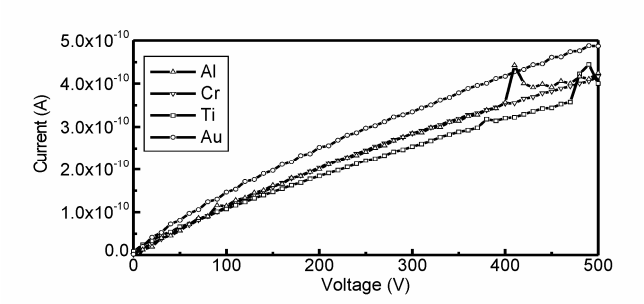

Fig. 3. I-V characteristics of the metal / AT-RB-1 / metal structure

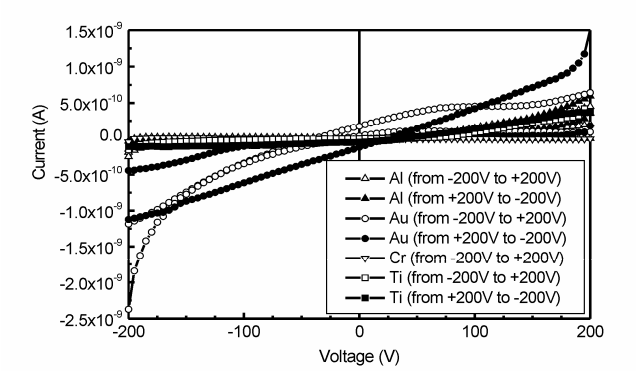

Fig. 4. I-V characteristics of the metal / AT-RB-2 / metal structure

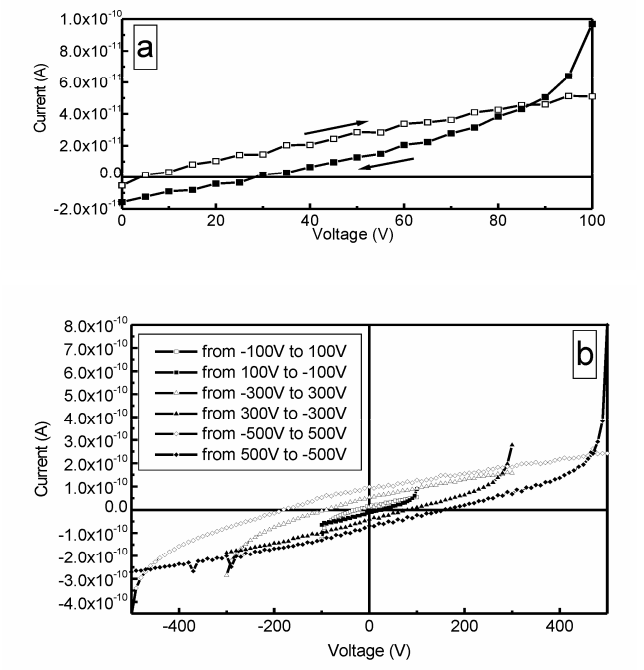

Fig. 5. Hysteresis of I-V characteristics of the Al / AT-RB-1 / Al structure in ±100 V (a) and ±300 V, ±500 V (b) voltage ranges

Table 2. Work functions of the metals used in present study (according to [10])

Metal	Al	Au	Cr	Ti
Work function (eV)	4.06 – 4.26	5.10 – 5.47	4.50	4.33

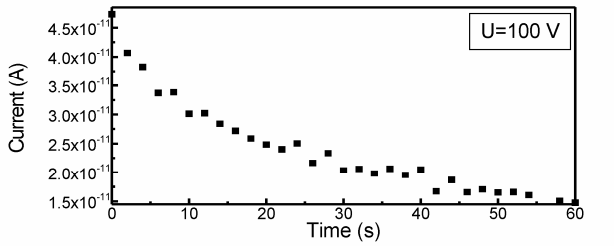

Fig. 6. The dependence of the current strength on time at constant voltage for metal / AT-RB-1 / metal structure

Effect of the hysteresis of the current-voltage characteristics was observed for all the samples fabricated using organic semiconductors MT-12, AT-RB-1, AT-RB-1 (air annealed) as well as E-139 (Fig. 5). Typical hysteresis of I-V characteristics for Al / AT-RB-1 / Al structure is presented in Fig. 5. The hysteresis was more pronounced when "bipolar" measurement of I-V characteristic (beginning from the some voltage ≠0 V) was performed instead of the unipolar measurement beginning with 0 V. Hysteresis of the I-V characteristic measured in ±100 V, ±300 V, ±500 V voltage ranges had the same shape, while difference between the currents measured during the "forward" and "back" measurements increased with increase of the voltage range. The difference between the "forward" and "back" current at the point of the maximum measurement voltage (Fig. 5) can be explained by change of the current density at the measurement voltage as it is shown in Fig. 6. It can be seen in Fig. 5, that at 100 V voltage after the 1 min current strength change as high as 3 times for metal / AT-RB-1 / metal structure was observed. It should be mentioned, that other authors reported about the I-V characteristic hysteresis effects in the case of the metal-organic semiconductor contacts, too (e. g., [11, 12]).

In the case of the samples fabricated using organic semiconductor AT-RB-2 hysteresis of the I-V characteristics is less pronounced (Fig. 4).

I-V characteristics of the Al / organic semiconductor / / Al and Cr / organic semiconductor / Cr samples fabricated using different organic semiconductors are presented in Fig. 7. In all cases I-V characteristics can be divided to the two groups. The smallest differences between I-V characteristics belonging to the different groups can be seen in the case of the MT-12 organic semiconductor. It can be mentioned, that in the case of the samples fabricated using organic semiconductor E-139 higher current were measured in comparison with the samples fabricated using organic semiconductor AT-RB-1. Data on hysteresis of the I-V characteristics in ±200 V range can be seen in Fig. 7, b. The highest currents and the biggest hysteresis of I-V characteristics were observed for samples fabricated using organic semiconductor E-139. While the lowest currents and weakest hysteresis of I-V characteristics effect were observed in the case of the metal / organic semiconductor / metal structures fabricated using organic

semiconductor MT-12. It should be mentioned, that in the case of the Al / AT-RB-2 / Al samples I-V characteristics were asymmetrical, diode-like (Fig. 7, c). While in the case of Cr / AT-RB-2 / Cr structures relatively weak currents were observed and absence of the hysteresis.

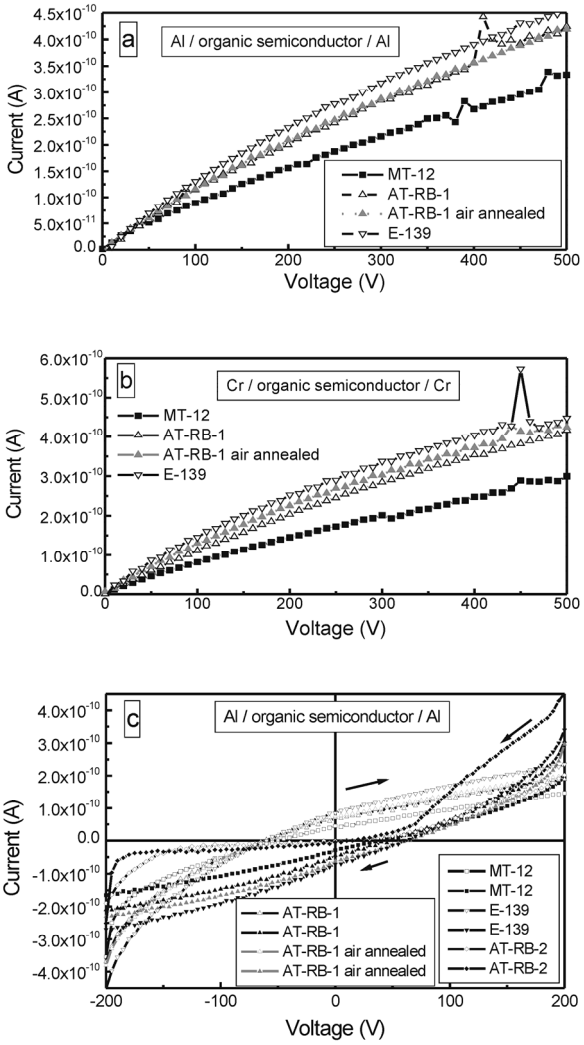

Fig. 7. I-V characteristics of metal / organic semiconductor / / metal structures fabricated using different organic semiconductors: electrode metal Al (a, c) and Cr (b). In c, d, pictures solid symbols refer to the measurement from –200 V to +200 V and hollow symbols refer to the measurement from +200 V to –200 V

3.2. Charge transfer mechanisms

In present study charge transfer mechanisms in metal/organic semiconductor/metal structures were studied. Linear and quasi-linear $I \sim U^{1/2}$ dependence ranges can be seen in Schottky plot for Al / organic semiconductor / Al structures (Fig. 8). However, only for highest voltages (electric field strength) dielectric permittivity value calculated from I-V characteristic was 2.3 – 2.7 – the value within the range of the dielectric permittivities reported in literature (according to [13 – 15] 1.5 – 8). In other cases unrealistically low values of the dielectric permittivity ($\varepsilon < 1$) was achieved.

Two tunnelling related charge transfer mechanisms – trap activated tunnelling (TAT) and Fowler-Nordheim emission were considered as well. It can be seen in Fig. 9, that TAT is possible charge transfer mechanism in our case. While there is no areas of the linear dependence $\ln(J/E^2) \sim E^{1/2}$ in Fowler-Nordheim plot (Fig. 10).

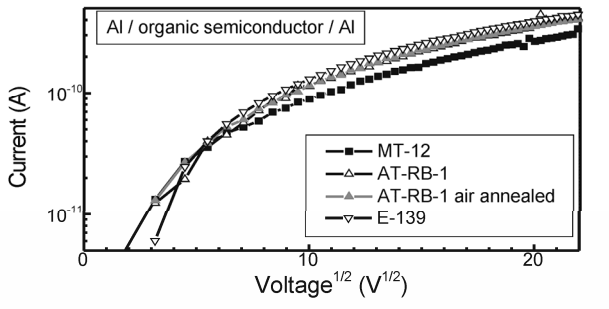

Fig. 8. Schottky plot of the I-V characteristics of Al / organic semiconductor / Al sample

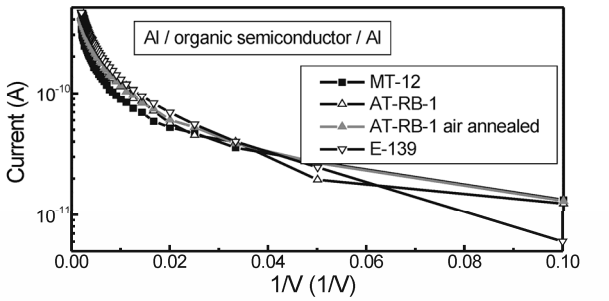

Fig. 9. TAT plot of the I-V characteristics of Al / organic semiconductor / Al sample

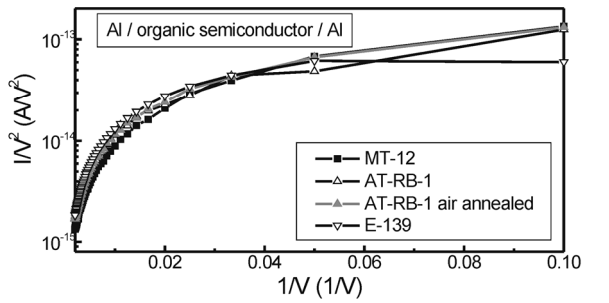

Fig. 10. Fowler-Nordheim plot of the I-V characteristics of Al / organic semiconductor / Al sample

In the case of the plots related with the bulk limited charge transfer mechanisms linear and quasi-linear areas can be seen in double logarithmic plot (Fig. 11). It is the behaviour typical for space charge limited current. It was mentioned above, that current density should depend on the distance between the electrodes in the case of the space charge limited currents. However, no dependence of the current density on distance between the electrodes was observed (Fig. 11, b). It means, that the space charge limited currents are not between the main charge transfer mechanisms in investigated samples. Poole-Frenkel plot is presented in Fig. 12. Some areas of the linear or quasilinear dependence of the $\ln(J/E) \sim E^{1/2}$ can be seen in it. However, dielectric permittivity values of the organic semiconductors calculated from the Poole-Frenkel plot were too low (<1) or unrealistically big (>1500).

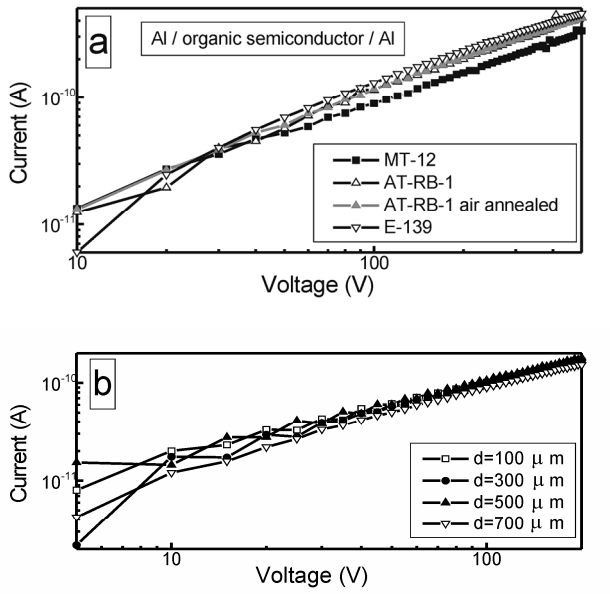

Fig. 11. Double logarithmic plot of the I-V characteristics of Al / organic semiconductor / Al samples (a) and Au / /E-139 / Au samples with different inter-electrode distance *d* (b)

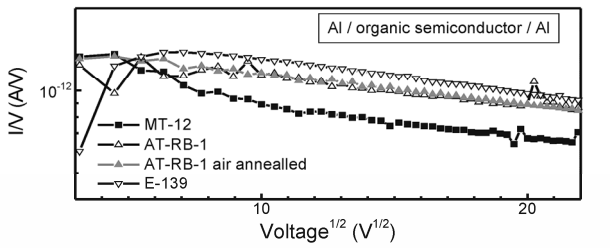

Fig. 12. Poole-Frenkel plot of the I-V characteristics of Al / organic semiconductor / Al sample

In general, the study revealed, that the main charge transfer mechanism in the investigated metal/organic semiconductor/metal samples is trap activated tunnelling. However, at higher voltages (electric field strengths) Schottky emission is possible as well. In such a case absence of the clear relation between the electrode metal workfunction and current-voltage characteristics of the samples can be explained by Fermi level pinning phenomena. Fermi level pinning was already reported for metal and organic semiconductor perylenetetracarboxyl dianhydride (PTCDA) contacts [16]. It can be mentioned, that two groups of I-V characteristics of the samples observed in the present study are close to the cases of the filled and free traps reported in [17] for organic light emitting diode I-V characteristics. In addition it can be noticed, that some authors reported about the bulk limited charge transfer mechanisms such as space charge limited currents in metal / organic semiconductor contacts [18]. However, in most cases contact limited charge transfer mechanisms were revealed: Schottky emission in [19], Fowler-Nordheim tunnelling (emission) in [20, 21], trap activated tunnelling in [17]. Formation of the electrically active traps observed in the present study can be explained by interaction between the organic semiconductor and metal during evaporation of the metal layer. E. g., there were stated in [20], that Au can diffuse into the organic semiconductor as deep as 10 nm.

3.3. Charge transfer mechanisms and I-V characteristic hysteresis effects

More detailed analysis of the hysteresis of I-V characteristic measured from –200 V to +200 V and backwards of the metal / organic semiconductor / metal sample is presented in Fig. 13, 14. Cr / E139 / Cr sample was choosed for analysis as a typical. It can be seen, that at the first trap activated tunnelling current flow through the sample. Some quasilinear dependence can be seen in Schottky plot in –200 V – –80 V voltages range (Fig. 13, a). However dielectric permittivity calculated from that part of the Schottky plot is unrealistically low (<0.2). I-V characteristic measured "forward" at the positive voltages range can be described by both trap activated tunnelling and Schottky emission currents. Values of the dielectric permittivity calculated from the Schottky plot are ~10 at low voltages, 3 – 3.5 at the medium voltages range and ~5.5 at the highest voltages range. It is within the dielectric permittivities reported for organic semiconductors by other authors range or close to it [13 – 15]. Backward measurement of the I-V characteristic (from +200 V to –200 V) results in the same charge transfer mechanisms as in the case of the measurement from –200 V to +200 V: at the first trap activated tunnelling current is observed. Afterwards charge transfer can be described by mixture of TAT and Schottky emission currents.

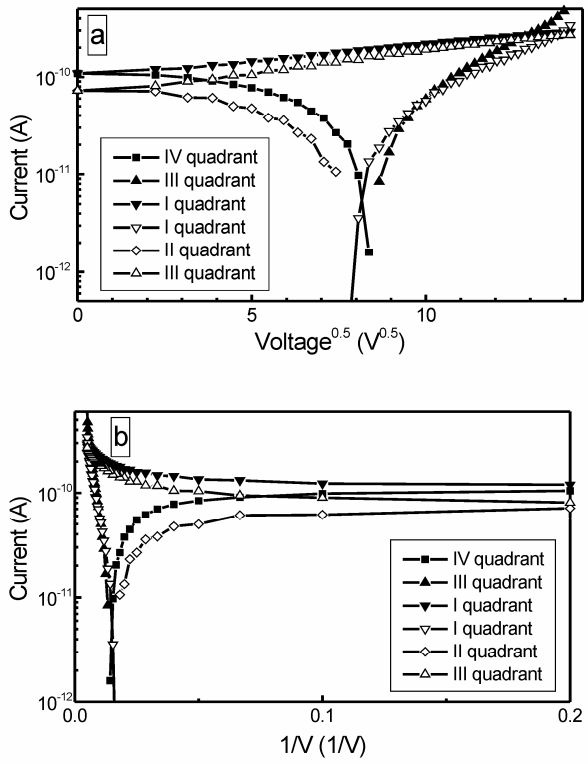

Fig. 13. Analysis of the hysteresis of I-V characteristic of Cr / / E-139 / Cr sample: Schottky plot with insert of the overall view with signed quadrants (a), TAT plot (b). Measured in from –200 V to +200 V (solid figures) and from +200 V to –200 V (open figures)

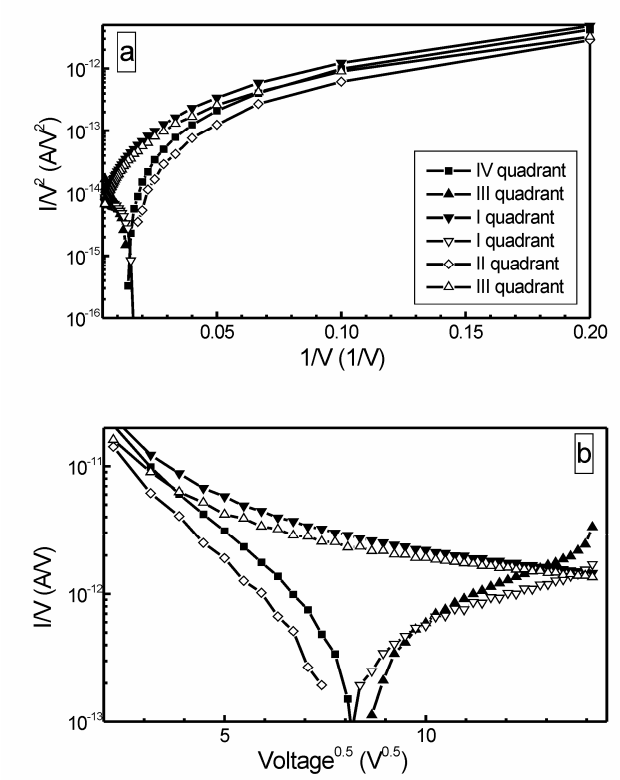

Fig. 14. Analysis of the hysteresis of I-V characteristic of Cr / / E-139 / Cr sample: Fowler-Nordheim plot (a), Poole-Frenkel plot (b). Measured in from –200 V to +200 V (solid figures) and from +200 V to –200 V (open figures)

CONCLUSIONS

In conclusion I-V characteristics of the metal / organic semiconductor / metal samples were studied. No clear relation between the electrode metal workfuntion and I-V characteristics of the metal / organic semiconductor contacts was observed. There were revealed, that current-voltage characteristics of the all samples fabricated using AT-RB-1, MT-12 and E-139 organic semiconductors and Ti, Al, Cr, Au metal electrodes can be divided into the two groups. For all the samples mentioned above I-V characteristic hysteresis effects were observed. The strongest hysteresis and largest current densities were observed in the case of the samples fabricated using E-139 organic semiconductor. While in the case of MT-12 organic semiconductor the weakest I-V characteristic hysteresis effect and smallest current densities were measured.

The main charge transfer mechanism in the investigated samples was trap activated tunnelling. At higher voltages (electric field strengths) Schottky emission should be considered as a possible charge transfer mechanism as well. In the case of the I-V characteristics hysteresis in ±200 V range there were revealed, that measuring from –200 V to +200 V at the first trap activated tunnelling current flow through the sample. While I-V characteristic measured at the positive voltages range can be described by both trap activated tunnelling and Schottky emission currents. Backward measurement of the I-V characteristic (from +200 V to –200 V) results in the same charge transfer mechanisms as in the case of the measurement from –200 V to +200 V: at the first trap activated tunnelling current is observed. Afterwards charge transfer can be described by mixture of TAT and Schottky emission currents. It should be mentioned, that in the case of the Al / AT-RB-2 / Al samples I-V characteristics were asymmetrical (diode-like) with big scattering from sample to sample. Therefore its analysis wasn't done.

Acknowledgments

Support of the Lithuanian Science and Studies Foundation in the frames of the High technologies development program project "Development and application of advanced holographic security means" (HOLOKID) is acknowledged. Authors would like to thank Albinas Svirskis (Institute of Materials Science of Kaunas University of Technology) for help in preparation of the equipment devoted to the measurement of I-V characteristics in nitrogen gas ambient.

REFERENCES

1. **Forrest, S. R.** The Path to Ubiquitous and Low-cost Organic Electronic Appliances on Plastic *Nature* 428 2004: pp. 911 – 918.
2. **Dimitrakopoulos, C. D., Malenfant, P. R. L.** Organic Thin Film Transistors for Large Area Electronics *Advanced Materials* 14 2002: pp. 99 – 117.
3. **Dimitrakopoulos, C. D., Mascaro, D. J.** Organic Thin-film Transistors: a Review of Recent Advances *IBM Journal of Research and Development* 45 2001: pp. 11 – 27.
4. **Misra, A., Kumar, P., Kamalasanan, M. N., Chandra, S.** White Organic LEDs and Their Recent Advancements *Semiconductor Science and Technology* 21 2006: pp. R35 – R47.
5. **Getautis, V., Gražulevičius, J. V., Malinauskas, T., Jankauskas, V., Tokarski, Z., Jubran, N. L.** Novel Families of Hole-transporting Monomers and Polymers *Chemistry Letters* 33 2004: pp. 1336 – 1337.
6. **Nomura, S., Nishimura, K., Shirota, Y.** Charge Transport in the Glassy State of Arylaldehyde and Arylketone Hydrazones *Thin Solid Films* 273 1996: pp. 27 – 34.
7. **Matoliukštyte, A., Burbulis, E., Gražulevičius, J. V., Jankauskas, J., Gaidelis, V.** Carbazole-containing Enamines for Electrophotography *Synthetic Metals* 158 2008: pp. 462 – 467.
8. **Gonon, P., Deneuville, A., Fontaine, F., Gheeraert, E.** Electrical Conduction and Deep Levels in Polycrystalline Diamond Films *Journal of Applied Physics* 78 1995: pp. 6633 – 6638.
9. **Houng, M. P., Wang, Y. H., Chang, W. J.** Current Transport Mechanism in Trapped Oxides: a Generalized Trap-assisted Tunneling Model *Journal of Applied Physics* 86 1999: pp. 1488 – 1491.
10. **Myburg, G., Auret, F. D., Meyer, W. E., Louw, C. W., van Staden, M. J.** Summary of Schottky Barrier Height Data on Epitaxially Grown n- and p-GaAs *Thin Solid Films* 325 1998: pp. 181 – 186.
11. **Takshi, A., Madden, J. D.** Large Apparent Inductance in Organic Schottky Diodes at Low Frequency *Journal of Applied Physics* 99 2006: pp. 084503-1 – 084503-5.
12. **Noh, Y. H., Park, S. Y., Seo, S., Lee, H.** Root Cause of Hysteresis in Organic Thin Film Transistor with Polymer Dielectric *Organic Electronics* 7 2006: pp. 271 – 275.

13. **El-Nahass, M. M., El-Deeb, A. F., Abd-El-Salam, F.,** Influence of Temperature and Frequency on the Electrical Conductivity and the Dielectric Properties of Nickel Phthalocyanine *Organic Electronics* 7 2006: pp. 261 – 270.
14. **Zang, D. Y., So, F. F., Forrest, S. R.** Giant Anisotropies in The Dielectric-Properties of Quasi-Epitaxial Crystalline Organic Semiconductor Thin-Films *Applied Physics Letters* 59 1991: pp. 823 – 825.
15. **Bobnar, V., Levstik, A., Huang, C., Zhang, Q. M.** Intrinsic Dielectric Properties and Charge Transport in Oligomers of Organic Semiconductor Copper Phthalocyanine *Physical Review Letters B* 71 2005: p. 041202(R).
16. **Agrawal, R., Ghosh, S.** Electrical Characterization of Fermi Level Pinning in Metal/3,4,9,10 Perylenetetracarboxylic Dianhydride Interfaces *Applied Physics Letters* 89 2006: pp. 222114-1 – 222114-3.
17. **Conwell, E. M., Wu, M. W.** Contact Injection into Polymer Light-emitting Diodes *Applied Physics Letters* 70 1997: pp. 1867 – 1869.
18. **Senthilarasu, S., Sathyamoorthy, R., Lalitha, S., Subbarayan, A.** Space Charge Limited Current Conduction in ZincPhthalocyanine (ZnPc) Thin Films *Solid-State Electronics* 49 2005: pp. 813 – 817.
19. **Deshmukh, S. H., Burghate, D. K., Akhare, V. P., Deogaonkar, V. S., Deshmukh, P. T., Deshmukh, M. S.** Electrical Conductivity of Polyaniline Doped PVC-PMMA Polymer Blends *Bulletin of Materials Science* 30 2007: pp. 51 – 56.
20. **Thakur, A. K., Mukherjee, D. M., Preethichandra, G., Takashima, W., Kaneto, K.** Charge Injection Mechanism Across the Au-poly,,3-hexylthiophene-2,5-diyl… Interface. *Journal of Applied Physics* 101 2007: p. 104508.
21. **Matsushima, T., Sasabe, H., Adachi, Ch.** Carrier Injection and Transport Characteristics of Copper Phthalocyanine Thin Films Under Low to Extremely High Current Densities *Journal of Applied Physics* 88 2006: p. 033508.

DOI: 10.5755/j02.ms.26067